Glucose Micro-Biosensor For Scanning Electrochemical Microscopy Characterization of Cellular Metabolism in Hypoxic Microenvironments

# Glucose Micro-Biosensor For Scanning Electrochemical Microscopy Characterization of Cellular Metabolism in Hypoxic Microenvironments

**Simona De Zio[a], Maila Becconi[a], Alice Soldà[a], Marco Malferrari[a], Andreas Lesch[b] and Stefania Rapino[*]**

*a Department of Chemistry "Giacomo Ciamician", University of Bologna, Via F. Selmi 2, 40126 Bologna, Italy*

*b Department of Industrial Chemistry "Toso Montanari", University of Bologna, Viale del Risorgimento 4, 40136, Bologna, Italy*

**Corresponding author at: Department of Chemistry "Giacomo Ciamician", University of Bologna, Via F. Selmi 2, 40126 Bologna, Italy. **E-mail address**: stefania.rapino3@unibo.it*

## Abstract

Mapping of the metabolic activity of tumor tissues represents a fundamental approach to better identify the tumor type, elucidate metastatic mechanisms and support the development of targeted cancer therapies. The spatially resolved quantification of Warburg effect key metabolites, such as glucose and lactate, is essential. Miniaturized electrochemical biosensors scanned over cancer cells and tumor tissue to visualize the metabolic characteristics of a tumor is attractive but very challenging due to the limited oxygen availability in the hypoxic environments of tumors that impede the reliable applicability of glucose oxidase–based glucose micro-biosensors. Herein, the development and application of a new glucose micro-biosensor is presented that can be reliably operated under hypoxic conditions. The micro-biosensor is fabricated in a one-step synthesis by entrapping during the electrochemically driven growth of a polymeric matrix on a platinum microelectrode glucose oxidase and a catalytically active Prussian blue type aggregate and mediator. The as-obtained functionalization improves significantly the sensitivity of the developed micro-biosensor for glucose detection under hypoxic conditions compared to normoxic conditions. By using the micro-biosensor as non-invasive sensing probe in Scanning Electrochemical Microscopy (SECM), the glucose uptake by breast metastatic adenocarcinoma cell line, with an epithelial morphology, is measured.

**Keywords**: scanning electrochemical microscopy, hypoxic microenvironments, cancer cell metabolism, glucose sensing, microelectrode, electrochemical transduction.

## 1. Introduction

Cancer cells produce ATP, which is the "ready-to-use" source of chemical energy in the cell, mainly through the glycolytic pathway, even in presence of oxygen and functioning mitochondria. This metabolic alteration of cancer cells is known as Warburg metabolism.[1] The metabolic changes that let cancer cells switch from mitochondrial respiration to aerobic glycolysis is induced by the specific features of tumor microenvironment and they are fundamental for their survival and proliferation.[2] Tumor tissues of different patients affected by the same kind of cancer but also a single tumor mass from the same patient often show heterogeneities in terms of histological [3] and phenotypical features.[4] Local differences in cellular metabolism and the presence of tumor areas with different metabolic patterns are intrinsically related to tumor heterogeneity. The study of solid tumor metabolic heterogeneity can be employed to predict tumor aggressiveness and to identify specific targets.[5] To this purpose it is necessary to detect the level of key metabolites (e.g. glucose and lactate) with high spatial resolution in order to identify local metabolic activities. Hypoxia, which is a reduced concentration of oxygen, *i.e.*, 2-8% compared to normoxic conditions (~21%), is a common feature of tumor masses, caused by the uncontrolled growth of cancer cells that quickly deplete oxygen and nutrition apported from regular blood vessels. Cancer cell adaptation to hypoxia involves molecular factors such as the hypoxia-induced transcription factor HIF-1.[6] Glycolysis was found to be increased in the most hypoxic regions of tumor masses.[7–9] Since tumor hypoxia is often associated with aggressive, resistant to therapies and highly metastatic tumor types, [10,11] the study of the correlation between hypoxia and cellular glycolytic metabolism may represent a crucial prognostic information. Over the years, many devices have been developed to perform spatially resolved measurements of metabolites, such as glucose, that are involved in cancer metabolic alterations. The simultaneous measurement of oxygen and glucose levels is important in cancer research, as this would allow for the characterization of metabolic activity of tumor cells in microenvironments with different oxygen levels and would be fundamental to understand the interplay between these factors. The principal

transduction strategies for glucose detection consist of optical [12–14] and electrochemical based biosensing devices. [15–18] For instance, amperometric electrochemical biosensors for glucose often employ electrodes (e.g. made of Pt) functionalized with the enzyme Glucose Oxidase (GOx). The functioning of these amperometric biosensors is based on the high specificity of GOx toward glucose and its ability to catalyze the oxidation of glucose to gluconolactone, using oxygen as co-substrate. Glucose is indirectly quantified by measuring the currents caused by the electrooxidation of hydrogen peroxide (secondary product of enzymatic reaction) at the working electrode. These biosensors, that rely on oxygen as co-substrate, present the disadvantage that they are inefficient when oxygen availability is too much limited in the analysis environment. This drawback becomes a challenge when micrometric biosensors are used to characterize the properties of cell cultures or biological microenvironments, in which oxygen is consumed by cell respiration. One strategy to overcome the oxygen limitation and enhance the detection sensitivity consists in including redox mediators in the active layers at the electrode surface.[19] In the GOx structure, the active FAD center is at about 13-18 Å from the surface of the enzyme [20] and the direct electron transfer between the $FADH_2$ group of the enzyme and the electrode surface results to be not possible. For this reason, the use of a redox mediator, entrapped within the enzyme containing layer, guarantees a faster electronic transfer between the redox center of the enzyme and the electrode. Numerous biosensors for glucose employing organic redox mediators have been proposed over the years, such as quinones and their derivatives [21], ferrocene [22] or pyridines. [23]. One of the most convenient strategies consists in the use of redox polymers able to communicate with the enzyme redox center and to avoid the common drawback of leakage of the mediator out of the sensing matrix; this leakage would implicate low durability of the biosensor performance and toxicity risk in case of implantable devices. However, the redox polymers generally require for the synthesis of the monomer molecules that are functionalized with the redox specie. [24,25] On the other hand, the surfaces of electrodes can be modified to enhance the electrode kinetics for the detection of redox active species that are created during the enzymatic reactions and whose concentration is proportional to that of glucose, such as $H_2O_2$. For instance, Prussian blue (PB) was widely used for the transduction of oxidase-based biosensing. Prussian blue and Prussian blue analogues (PBAs) possess a unique hexacyanometalate framework structure in which two iron atoms have different valences, *i.e.*, $Fe^{II}$ and $Fe^{III}$. The fully oxidized form of PB is known as Berlin green and the fully reduced form Prussian white. Prussian white has a catalytic activity toward $O_2$ and $H_2O_2$

reduction, while Berlin green (the oxidized form of PB) also acts on the $H_2O_2$ oxidation.[26] Prussian blue in nanoscale size can act also as nanozyme, a material with enzymatic-like catalytic properties and numerous advantages in stability, durability and costs; in particular PB can mimic three important classes of enzymes (e.g. peroxidase, catalase and superoxide dismutase) due to the various redox potentials of its forms, making it applicable in the field of biosensing, biotechnology and environmental treatment [27]. In glucose biosensors based on $H_2O_2$ detection, PB and its derivatives are widely used. [28–30] GOx and other active biosensor compartments must be immobilized on the electrode, *e.g.*, by using a polymer-based matrix. Several matrices can be employed to immobilize the enzyme at the electrode surface for amperometric biosensing [31,32]. Poly(3,4-ethylenedioxythiophene) (PEDOT) represents one candidate to construct very stable polymeric films for glucose biosensors.[33] Polypyrrole is the most often used polymer for this purpose thanks to the reproducible fabrication, simple polymerization processes and the high water-solubility of the monomer pyrrole.[34,35] This guarantees the growth of the polymer in aqueous buffers without the need of surfactants (*e.g.*, polyethylene glycol, polystyrene sulfonate), which is fundamental to retain the enzyme functionality. In this respect, Rekertaitė *et al* developed a glucose biosensor based on a graphite electrode modified with PB, GOx and polypyrrole. Some years later, the same authors designed other two types of glucose biosensors, based on PBAs, glucose oxidase and polypyrrole, introducing the Ni-hexacyanoferrate (NiHCF) and the Co-hexacyanoferrate (CoHCF) ions inside the electrode functionalization layer.[36,37] Bartlett *et al* [38] immobilized GOx in poly(N-methylpyrrole) films containing the ferrocyanide/ferricyanide redox couple onto a Pt macro-electrode. In order to explore microdomains, such as single cell microenvironment, microelectrodes can be used in Scanning Electrochemical Microscopy (SECM). [39–41] SECM is a powerful technique enabling functional imaging of substrates in solution with high spatial and temporal resolutions. An amperometric microelectrode is used to record a faradaic current as result of the presence of redox-active species in solution. If the microelectrode is positioned in close proximity to a substrate surface, the recorded current depends on both the topography and the electrochemical activity of the surface itself that affects the diffusion of the redox active species as well as their redox state.[42–44] Biological applications of SECM [17][45,46] include imaging of the flux of molecules in the proximity of the cell membrane, local chemical reactivity and metabolite concentrations, but also the possibility to scan the surface of a single living cell while electrochemically monitoring the activity associated with its metabolic

changes. [17][46–48] SECM can be applied to investigate the integrity of cell membranes of human myocardium-derived mesenchymal stem cells (hmMSC), highlighting the differences between healthy and pathological hmMSCs [45, 46]. It can be coupled with other techniques, such as atomic force microscopy (AFM), electrogenerated chemiluminescence (ECL) or fluorescence spectroscopy (FS). SECM was further combined with electrochemical impedance spectroscopy (EIS) to characterize the redox activity of immobilized active and inactivated yeast cells. [37]

In this work, the development and application of an amperometric glucose micro-biosensor is presented, which is able to detect glucose in hypoxic microenvironments, defined as oxygen pressures ranging from 2%-8% (~2.02 KPa-8.08 KPa), with high spatial resolution. The micro-biosensor is based on an electrochemically generated film comprising polypyrrole, ferricyanide/ferrocyanide and GOx, deposited on a Pt microelectrode of 10 µm. We report on the methodology for the preparation of the biosensor and on the characterization of the microbiosensor under hypoxic as well as normoxic conditions. Furthermore, we present the use of the micro-biosensor as probe of SECM to characterize single-cell glycolytic activity in hypoxic microenvironment, by recording glucose levels with high spatial resolution together with the assessment of the oxygen concentrations.

## 2. Materials and methods

**2.1 Materials.** Glucose Oxidase (GOx) type X-S (EC 1.1.3.4. from Aspergillus Niger, Merck), $K_3[Fe(CN)_6]$ (Sigma), D-(+)-glucose (Sigma), phosphate buffer (pH 6.3 from Merck), Phosphate-Buffered Saline 1x (pH 7.4) (Microtech), pyrrole 98% (Merck), paraformaldehyde (PAF) ≥ 95.0% (Merck) and glycine >99% (Merck) were purchased were used as received. Dulbecco's Modified Eagle's Medium-low glucose (DMEM, from Microtech) was supplemented with 10% Fetal Bovine Serum, 1% Penicillin/Streptomycin and 1% L-glutamine.

**2.2 Electrochemical Instrumentation.** All electrochemical measurements were carried out with an electrochemical workstation 910B SECM (CH Instruments) coupled with a Nikon ECLIPSE *Ti* (phase contrast and fluorescence) inverted optical microscope enabling electrochemical and optical microscopic characterizations in identical coordinates. The stepper motors and the

piezoelectric components of the 910B CHI instrument for the microelectrode positioning were removed from the original stage and mounted on the plate of the inverted microscope.

**2.3 Electrochemical cell and electrodes.** Electrochemical procedures were carried out in three-electrode configuration, comprising a microelectrode (ME) with 10 µm diameter Pt disk (CHI116 10 µm diameter Pt SECM tip, indicated as "T") as working electrode (WE), a platinum wire as counter electrode (CE) and a Ag/AgCl (KCl 3 M) (CHI Ag/AgCl Reference Electrode w/ porous Teflon Tip) or a Ag wire as reference electrode (RE). The ME was polished prior to its use with abrasive diamond paper on a glass support, followed by sonication for some seconds in a bath sonicator. Counter and quasi-reference electrodes were polished with alumina (diameter 1 µm and 0.05 µm) and DI water before their use. Petri dishes were used as electrochemical cells. Hypoxic conditions (*i.e.*, oxygen concentration between 2% and 8%) were obtained by the controlled purging with argon. The oxygen concentration was verified from voltametric measurements in unstirred solution.

**2.3 Preparation of the glucose micro-biosensor.** The micro-biosensors were prepared in a single step. For the preparation of the glucose micro-biosensor, 2 mg of GOx were dissolved in 1 mL of phosphate buffer (pH 6.3) containing 0.1 M potassium ferricyanide. Pyrrole was added to the resulting solution as last component to a final concentration of 0.1 M and the solution was de-oxygenated. The polymeric film was then potentiostatically grown at 900 mV *vs.* Ag quasi-RE for 15 min. The resulting composite film on the Pt MEs contained entrapped GOx, a ferrocyanide/ferricyanide-Prussian Blue type (PBT) precipitate and polypyrrole (PPyr), which is denoted as PPyr-GOx-PBT/Pt microelectrode. For the preparations of PBT/Pt ME, PPyr-PBT/Pt ME and PPyr-GOx/Pt ME, the same protocol was applied, without adding pyrrole, GOx and potassium ferricyanide, respectively, to the electropolymerization solution. The as-obtained electrodes were washed with MilliQ water and stored at 4 °C until their use.

**2.4 Electrochemical characterizations.** Standard electrochemical methods have been applied for sensor characterization. Cyclic Voltammetry (CV) and amperometric calibrations (amperometric *i-t* curves) were performed in phosphate-buffered saline (PBS, pH 7.4) and DMEM culture medium, both under atmospheric oxygen pressure (*i.e.*, normoxic conditions) or after purging with Argon (to realize hypoxic and anoxic conditions). A silicon rubber shield was used on top of the

cell to prevent oxygen diffusion from the environment into the electrochemical cell during measurements. Amperometric measurements were carried out in PBS under stirring.

**2.5 SECM measurements of cell cultures.** About 50.000 MDA-MB-468 cells (ATCC: HTB-132) were cultured in Dulbecco's Modified Eagle's Medium (DMEM) with 5.5 mM glucose inside 35 mm diameter Petri dishes. For control experiments, about 50.000 MDA-MB-468 cells (ATCC: HTB-132) were fixed inside 35 mm diameter Petri dishes by first washing the cells three times with PBS (300 µL each) and second by adding 200 µL of PAF with exposure time of 10 min at room temperature. Third, PAF was neutralized by washing the fixed cells three times for 5 minutes with 300 µL of glycine 0.1% in PBS. The fixed cells were then maintained in PBS until replaced by DMEM with 5.5 mM glucose for the SECM measurements. The Petri dish was thereafter mounted on the plate holder of the inverted microscope and covered by a micro-incubation system, with which it was possible to maintain the cell culture conditions also during the electrochemical analyses (temperature 37°C, $CO_2$ flow 0.04 L/min, air flow 0.8 L/min). The DMEM culture medium could be de-oxygenated or contained ambient oxygen pressure on demand. For the SECM measurements, the working potential $E_T$ was set to +0.75 V *vs* Ag quasi-RE. Approach curves, *i.e.*, the vertical approaching of the ME towards the bottom of the Petri dish, were recorded with a translation rate of 1.7 µm/s. Horizontal line scans were performed at constant height, reporting the working distance in respect to the bottom of the Petri dish. The translation rate was equal to 8.3 µm/s. For SECM imaging, *i.e.*, scanning the ME at constant height in the *x*,*y*-plane over a cell culture, the translation rate was 17 µm/s. The scans were treated using MIRA software by Prof. Wittstock (https://uol.de/pc2/forschung/secm-tools/mira).

## 3. Results and Discussion

### 3.1 Fabrication of a PPyr-GOx-PBT/Pt microelectrode via electrochemical polymerization of pyrrole

The fabrication of the glucose microsensor for glucose measurements under hypoxic conditions was realized in one facile step. It was electrochemically prepared on a Pt ME in phosphate buffer solution containing 2 mg/mL GOx, 0.1 M potassium ferricyanide and 0.1 M pyrrole, pH 6.3. First, CVs were recorded between -0.7 V and 0.0 V *vs.* Ag quasi-RE. The ME was then approached to the bottom of the electrochemical cell with $E_T$ = 0 V, a procedure that generally took 100 s. Thereafter, the reaction solution was de-oxygenated (*i.e.*, removal of oxygen) as required for the electrosynthesis of PPyr [50]. Being positioned close to the bottom of the cell, the environment of the polymerization process was better controlled in terms of the diffusion of the reagents and absence of oxygen. Thereafter, a static potential of 0.9 V was applied for 900 s with the primary aim to electropolymerize pyrrole to polypyrrole (PPyr) (Supporting information **SI-1, Fig. S1**). The as-synthesized PPyr film during the electropolymerization was positively charged promoting the electrostatically driven incorporation of GOx (negatively charged at pH 6.3) [51] and of $[Fe(CN)_6]^{3-}$. For its characterization, the micro-sensor was washed with MilliQ water and immersed into hypoxic PBS (pH 7.4). **Fig. 1a** shows a cyclic voltammogram (CV) of the as-obtained electrode (curve 1). At about 0.6 V, an oxidation wave can be obtained while below -0.1 V a reduction wave sets in, which forms a plateau starting from -0.4 V. In order to get information about the composition and properties of the electro-synthesized film, alternative electrodepositions on cleaned Pt were carried out, in which the deposition solutions of de-oxygenated phosphate buffer (pH 6.3) contained i) only pyrrole, ii) pyrrole + ferricyanide and iii) only ferricyanide. The curves in **Fig. 1b** show the voltammetric characterization of the three as-obtained films in de-oxygenated PBS. The CV using PPyr/Pt (Fig. 1b, curve 1) does not show any significant redox peaks. In presence of pyrrole and ferricyanide during the electrodeposition the resulting film shows oxidation and reduction waves similar to those shown in curve 1 in Fig. 1a, even if they are shifted towards positive potentials. This suggests that the film formation is unaffected by the presence of GOx. In the presence of only ferricyanide during electrodeposition, the CV shows a pronounced oxidation peak with a minor reduction peak at about 0.1 V and an increasing cathodic current in the cathodic scan below -0.5 V, indicating an iron-based deposit on the Pt surface (Fig. 1b, curve

3). Notably, the presence of pyrrole during electrodeposition in ferricyanide containing PBS results in a film with significantly different redox properties than the one obtained without pyrrole. In further electrochemical characterization studies, the electrocatalytic properties towards the oxidation of ferrocenyl methanol and the reduction of ferricyanide in solution were investigated when the electrodeposited PPyr film contained the ferricyanide derivate (**SI-2**). The results suggest the presence of an electrocatalytically active material (**Fig. S2**) apart from electrostatically embedded ferricyanide. Taking into account the procedures used, we assume the presence of Prussian Blue (PB) or a similar material as electrocatalytically active deposit. Typically, PB particles and films on electrodes are electrochemically synthesized in acidic solution containing ideally ferrocyanide and a Fe(III) salt, such as $FeCl_3$. Acidic conditions cannot be applied in our approach, as GOx would be inactivated. Although higher pH values and PB precursor solutions different from the ideal one are disadvantageous for the formation of Prussian Blue [28,52], PB films haven been electrodeposited under mild acidic conditions on Pt in solutions containing only ferricyanide [53]. Among many different ways of preparation of PBTs, the single-source method consists in potassium ferricyanide solution as the single iron source; the mechanism is descripted as partial decomposition of $[Fe(CN)_6]^{3-}$ and further reduction of $Fe^{3+}$ at the electrode to allow the coordination of ferrous ion with ferricyanide to obtain PB [53,54]. This process may be accomplished chemically or electrochemically. Both procedures are based on a single ferricyanide compound dissociation, and they guarantee the formation of ultrathin PB/PBTs films, due to the low concentration of free ferric ions in solution. It can be assumed that ferricyanide ions dissociate during the CVs as well as approach curves that were performed before the electropolymerization of pyrrole. Furthermore, ferricyanide and pyrrole can react chemically in solution leading to ferrocyanide and oxidized pyrrole [55]. In fact, a greenish precipitate was observed when both ferricyanide and pyrrole were present in the solution. The PBT material is therefore probably formed due to the co-presence of ferrocyanide and ferricyanide and promoted by the local decrease of pH during the electropolymerization process of pyrrole. The PBT compound, in the form of nanoparticles or microparticles, is probably present also in the polymer matrix and not only on the electrode surface. Recording CVs of the PPyr-PBT/Pt ME and the PPyr/Pt ME in de-oxygenated 1 mM $H_2O_2$ and PBS (pH 7.4) confirmed the electrocatalytic effect of the deposited film towards $H_2O_2$ oxidation and reduction (**Fig. S3**). The presence of a Prussian Blue type material can therefore be suggested even though the CV of the film in PBS does not show the typical oxidation

and reduction peaks [56]. Instead, the signals found for the reduction of ferricyanide, added after electrodeposition to the solution, and oxidation of as-generated ferrocyanide appear very similar to the ones of the PPyr-based iron containing film, suggesting therefore the presence of ferricyanide inside the immobilized film on the ME (**Fig. S4**). From these observations, we conclude that a mixed PBT/embedded ferricyanide polymeric matrix could have been synthesized. The amount of PBT in direct contact with the platinum surface is probably very low compared to ferricyanide, impeding therefore the visibility of PB redox peaks in the CVs. For simplicity, we indicate the presence of the redox mediator mixture as "PBT", reminding however that it is most likely a mixture of PBT and ferricyanide. These first biosensor characterizations indicate that both $Fe^{2+}$ and $Fe^{3+}$ are present in the generated film, because in the CVs of the PPyr-PBT/ME in PBS plateaus are seen for both the oxidation and reduction of $Fe^{2+}$ and $Fe^{3+}$ species, respectively.

Thereafter, the electrocatalytic property of the PPyr-PBT/Pt ME for the determination of glucose was evaluated. Curve 2 in Fig. 1a shows the CV recorded with the PPyr-GOx-PBT/Pt ME in presence of 5 mM $\beta$-D-glucose in hypoxic PBS. Compared to the CV in the absence of glucose (Fig. 1a, curve 1), an electrocatalytic effect for the detection of glucose can be seen. For the oxidation as well as for the reduction the signals show higher currents and are shifted to lower overpotentials. The oxidation of glucose in the presence of oxygen as co-substrate is catalyzed by the oxidized form of GOx (GOx-FAD, "$GOx_{ox}$") giving gluconolactone and the reduced form of GOx (GOx-$FADH_2$, "$GOx_{red}$"). The oxidation of GOx-$FADH_2$ back to GOx-FAD is realized by oxygen leading to hydrogen peroxide. Hydrogen peroxide can be electrochemically oxidized or reduced depending on the electrode potential applied and electrocatalytic electrode material prepared. In fact, PB is a very well-known electrocatalyst for both the reduction as well as the oxidation of $H_2O_2$. Selecting the hydrogen peroxide reduction process can cause interferences with oxygen reduction. A redox mediator, such as ferricyanide, carries the electrons between the reduced form of GOx and the positively biased WE, in particular at low oxygen concentrations. Therefore, both $H_2O_2$ and redox mediator conversion can take place at the electrode for sensing. This is addressed in more detail in the following section.

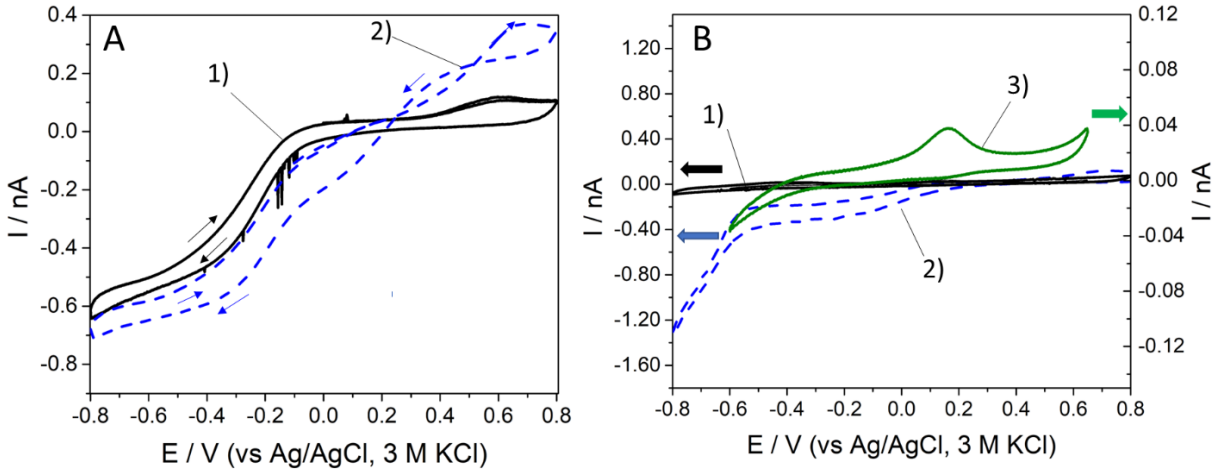


**Fig. 1.** a) Cyclic voltammograms of the PPyr-GOx-PBT/Pt microelectrode recorded in hypoxic PBS (pH 7.4) in absence (curve 1) and in presence (2) of 5 mM *β*-D-glucose. b) Cyclic voltammograms of a Pt microelectrode to which the electrodeposition procedure was applied in presence of pyrrole (1), pyrrole and ferricyanide (2) and only ferricyanide (3) recorded in hypoxic PBS (pH 7.4). Potential scan rate 20 mV/s, CE = Pt wire, RE = Ag/AgCl (KCl 3 M) reference electrode. Hypoxic conditions were realized by purging of the test solution with argon.

### 3.2 Quantitative response of the PPyr-GOx-PBT/Pt micro-sensor to glucose

The quantitative response of the PPyr-GOx-PBT/Pt ME towards glucose in PBS (pH 7.4) was thereafter analyzed under hypoxic conditions (**Fig. 2a**, black line) and compared with the responses of the PPyr-GOx/Pt ME (blue line) and PPyr-PBT/Pt ME (grey line). By applying a constant electrode potential, *i.e.*, +0.65 V vs. Ag/AgCl (3 M KCl), the currents were recorded over time while frequent additions of a glucose stock solution were carried out. The glucose concentration was iteratively increased ranging from 1 mM to 7 mM, which corresponds to physiological glucose concentrations in cancer tissues and is important for cancer cell studies under hypoxic conditions (*vide infra*). In the amperogram, current plateaus are formed that were the result of the hemispherical diffusion of reactants towards the modified ME and solution stirring during the glucose additions. In presence of GOx, the recorded currents increased after each addition of glucose. On the contrary, in the absence of GOx in the ME coating no changes in the recorded currents were observed by adding glucose, demonstrating that the developed sensor works as an enzymatic glucose biosensor and neither PPyr nor the PBT convert glucose directly. The calibration graphs, obtained by linear regression of the averaged plateau currents (**Fig. 2b**)

demonstrate that the sensitivity (*i.e.*, the slope of the linear calibration line) of the PPyr-GOx-PBT/Pt ME under hypoxic conditions was about 3.4 times higher than for the microsensor without PBT material (values shown in **Fig. 2b**). The response time of the micro-biosensor, *i.e.*, the time after a glucose addition until 90% of the plateau current was reached, was found to be 6-10 seconds (**SI-5**). The limit of detection (LOD, calculation in **SI-6**) of the micro-biosensor for glucose detection was 0.495 mM. Under hypoxic conditions, the oxygen availability is limited, which on the one hand favors GOx activity [57] and on the other hand the electron shuttling via redox mediators, such as Fe(III)-containing species. [58] The redox mediators carry electrons from the reduced form of GOx to the anodically biased electrode.

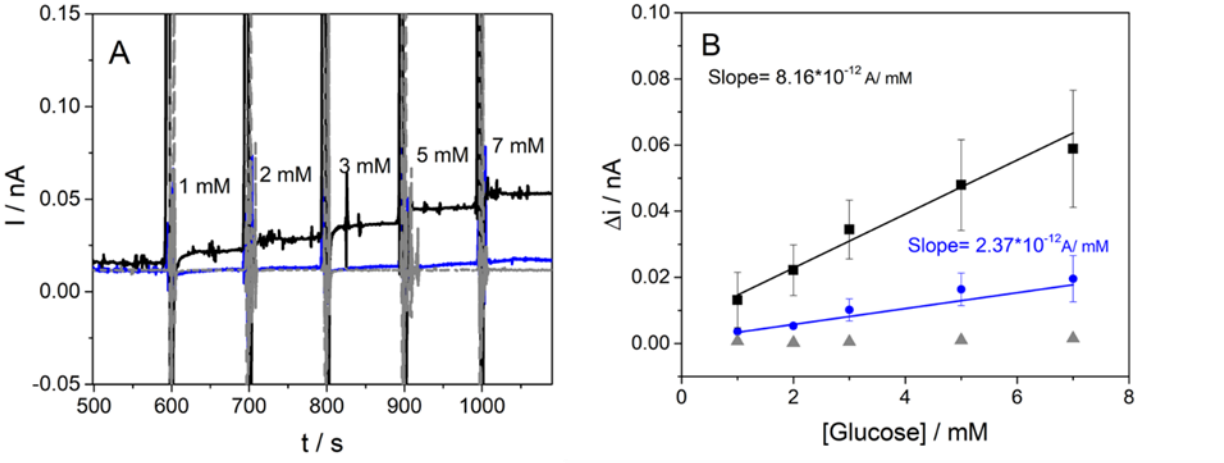


**Fig 2.** a) Amperometric responses of one PPyr-GOx-PBT/Pt ME (black line), one PPyr-GOx/Pt ME (blue line) and one PPyr-PBT/Pt ME (grey line) upon subsequent additions of D-glucose to PBS between 1 mM and 7 mM (pH 7.4) under hypoxic conditions. Hypoxic conditions were realized by purging of the test solution with argon. Applied potential = +0.65 V *vs.* Ag/AgCl (3 M KCl). b) Resulting calibration lines obtained from the amperometric responses of PPyr-GOx-PBT/Pt ME (black line) and PPyr-GOx/Pt ME (blue line) shown in (a). Error bars show standard errors for each concentration value measured with three different micro-biosensors for each sensor type.

The performance of the glucose micro-biosensor under hypoxic conditions was then compared to its performance under atmospheric oxygen pressure (that we call hereafter normoxic condition) using amperometry with increasing concentrations of glucose between 1 mM and 5 mM (**Fig. 3a**). The applied electrode potential is supposed to oxidize ferrocyanide, which was formed by the electron transfer from ferricyanide to the reduced form of GOx. As it can be seen from the calibration graphs (**Fig. 3b**), the sensitivity of the glucose micro-biosensor reduces by a factor of

2.3 in the presence of ~21% oxygen. Oxygen as physiological electron acceptor can compete with or even outperform redox mediators, such as ferricyanide, in enzymatic glucose sensing for the oxidation of GOx-$FADH_2$ to GOx-FAD, generating therefore preferably $H_2O_2$ instead of ferrocyanide. The presence of the PBT material also enables the electro-oxidation of $H_2O_2$ as a measure of glucose concentration. As consequence, less ferrocyanide formation could result in lower anodic currents for the same concentration of glucose. Furthermore, it has been reported that the catalytic efficiency of GOx increases under hypoxic conditions [57]. The electrocatalytic oxidation of hydrogen peroxide by the PBT material together with the higher efficiency of GOx for glucose oxidation may increase the efficiency towards glucose detection under hypoxic conditions. As a result, the performance of the prepared glucose microsensor is clearly affected by the concentration of oxygen in the microenvironment. The behavior of the micro-biosensor under normoxic condition highlights the micro-biosensor's poor performance in catalyzing glucose oxidation reaction when oxygen is present at ~21%. Glucose oxidase expresses its maximum efficiency for glucose oxidation when the oxygen level is low [57]. The enzymatic turnover is inversely proportional to the oxygen partial pressure $pO_2$ and a high turnover is therefore obtained when $pO_2$ is about 10-15 kPa, which corresponds to an oxygen level of ~10%.[57]

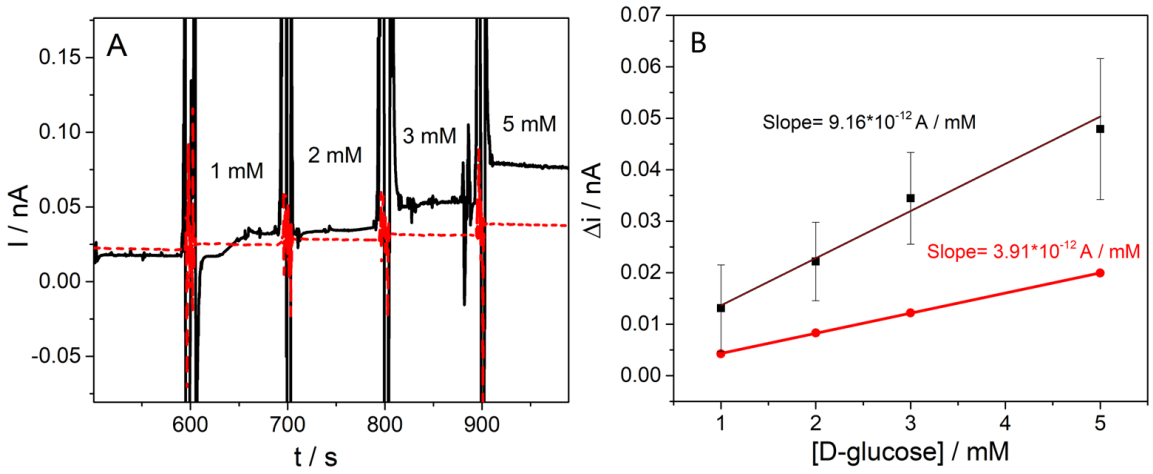


**Fig 3**. a) Amperometric response of PPyr-GOx-PBT/Pt micro-biosensor upon subsequent additions of D-glucose between 1 mM and 5 mM in PBS (pH 7.4) under hypoxic conditions (black) and normoxic conditions (red trace). Applied potential: +0.65 V *vs.* Ag/AgCl (3 M KCl). b) Resulting calibration lines obtained from the amperometric responses of the PPyr-GOx-PBT/Pt micro-biosensor at glucose additions in PBS under hypoxic conditions (black lines and points, $R^2$= 0.996, error bars show standard errors for each concentration value measured with three different micro-biosensors) and normoxic conditions (red lines). Hypoxic conditions were realized by purging of the test solution with argon.

The superior performance of the fabricated micro-biosensor under hypoxic conditions was further evaluated using cyclic voltammetry (**Fig. 4**). **Fig. 4a** shows the CVs recorded with the PPyr-GOx-PBT/Pt micro-biosensor in PBS (pH 7.4) under normoxic (blue curve 2) and hypoxic (black curve 1) conditions. The anodic and cathodic signals seen under hypoxic conditions are most likely due to the presence of ferricyanide in the electrode coating (*vide supra*). Notably, the electrode film related signals under hypoxic conditions were stable during the time course of the measurements carried out in this work indicating that ferricyanide does not leak out of the electrode coating (**Fig. S7**). Under normoxic conditions, a wave for the oxygen reduction reaction, starting at 0.1 V *vs.* Ag/AgCl (3M KCl) in the cathodic scan and forming a plateau at -0.6 V, can be seen clearly (blue curve 2) while only capacitive currents are seen in the anodic region of the CV. In presence of 5 mM glucose in hypoxic PBS (**Fig. 4b**), the PPyr-GOx-PBT/Pt ME shows a catalytic anodic response for glucose (black curve 1), which is substantially weaker under normoxic conditions (blue curve 2). The experimental observations could indeed confirm the enhanced kinetics of glucose oxidation by GOx as well as the favored electron transport by the ferricyanide/ferrocyanide-based mediator between GOx and positively biased Pt electrode when being operated under hypoxic conditions (*i.e.*, 2-8% oxygen). In the cathodic region of the CV, changes in the electrode signal under hypoxic conditions are minor, while under normoxic conditions the cathodic current due to oxygen reduction is significantly superimposed by a signal that most likely is due to the reduction of hydrogen peroxide, see also **SI-8**. On the other hand, the micro-sensors show cathodic currents that are dominated by the reduction of oxygen. Therefore, the micro-biosensor can also be used in a dual mode for glucose and oxygen detection dependent on the electrode potential (**Fig. S8**).

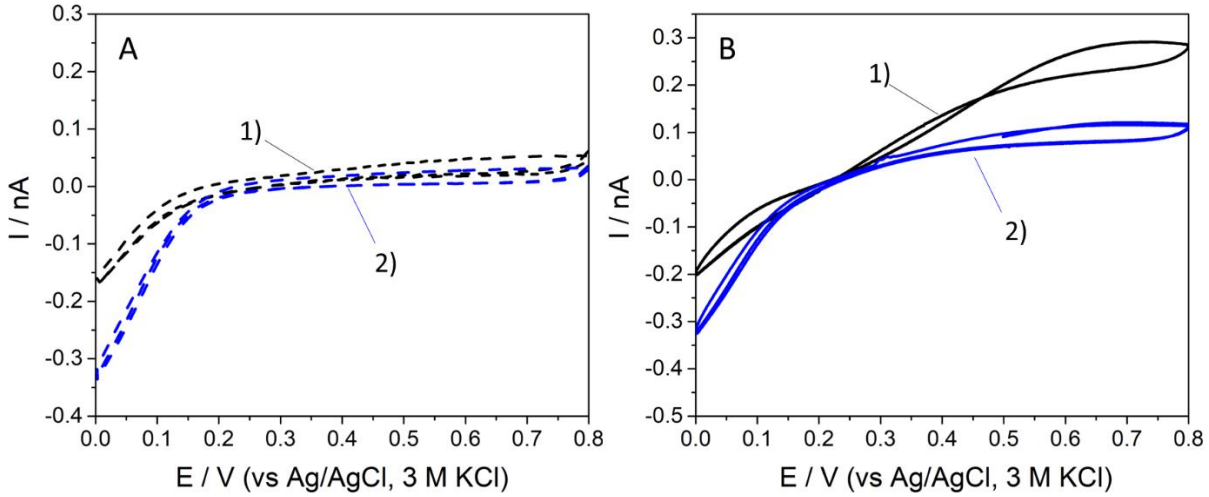


**Fig. 4**. a) CVs recorded with PPyr-GOx-PBT/Pt ME in PBS (pH 7.4) under hypoxic (1) and normoxic (2) conditions. b) CVs recorded with PPyr-GOx-PBT/Pt ME in PBS (pH 7.4) containing 5 mM glucose under hypoxic (1) and normoxic (2) conditions. Potential scanned between -0.8 to 0.8 V vs Ag/AgCl (3 M KCl) reference electrode, CE = Pt wire. Scan rate: 20 mV/s. Hypoxic conditions were realized by purging of the test solution with argon.

Based on the experimental observations discussed above, the functionality of the micro-biosensor is most likely based on the combination of the two possible mechanisms shown in **Scheme 1**, *i.e.*, ferrocyanide/ferricyanide-mediated or $H_2O_2$ detection-based, which depend on the concentration of oxygen in the environment.

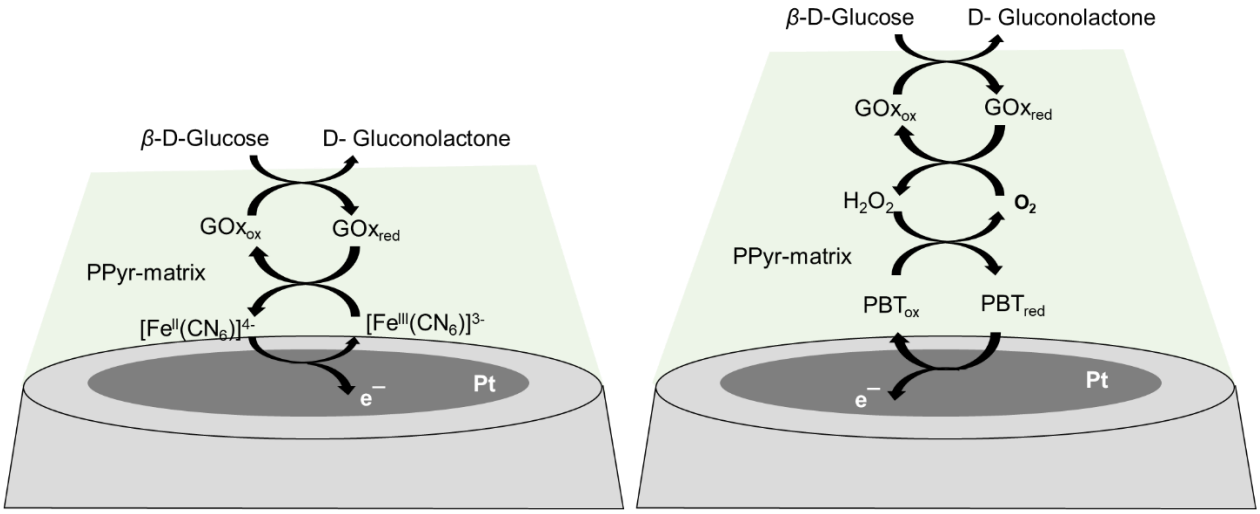


**Scheme 1.** Schematic representation of the suggested reactions involved in the detection of glucose using the PPyr-GOx-PBT-based glucose micro-biosensor.

### 3.3 Glucose metabolic consumption of single tumor cells in hypoxic microenvironment

The PPyr-GOx-PBT/Pt ME as glucose micro-biosensor was then used as SECM probe to measure the metabolic glucose uptake at the single cell level of cancer cells. The breast cancer line MDA-MB-468 was investigated, because this cell line is known as a typical cellular model of triple negative breast cancer, characterized by a glycolytic metabolism. The cells were kept in DMEM medium containing 5.5 mM glucose. Firstly, the PPyr-GOx-PBT/Pt ME was vertically approached from the bulk of the initially normoxic medium towards the bottom of the Petri dish using an SECM approach curve. A tip potential of +0.75 V *vs.* Ag quasi-RE was applied for glucose detection. While approaching the ME towards the bottom of the Petri dish, the substrate surface below the tip, at a certain distance, initiates to block the diffusion of glucose as well as of oxygen towards the active part of the micro-biosensor. As consequence, the recorded current changes, which allows the estimation of the height of the micro-biosensor over the Petri dish. The approach curve is shown in **Fig. 5a**, which was created by plotting the normalized tip current, which is the recorded current at each coordinate divided by the tip current in solution bulk, as a function of the working distance,. As it can be seen, the recorded current remained constant in the solution bulk until a working distance of about 300 µm. With decreasing oxygen availability, the recorded tip current increased. This confirms that the glucose micro-biosensor performance becomes more sensitive at reduced local oxygen concentrations. Once the micro-biosensor was positioned inclose proximity to the bottom of the Petri-dish, the cell medium was partially degassed to create the hypoxic environment.

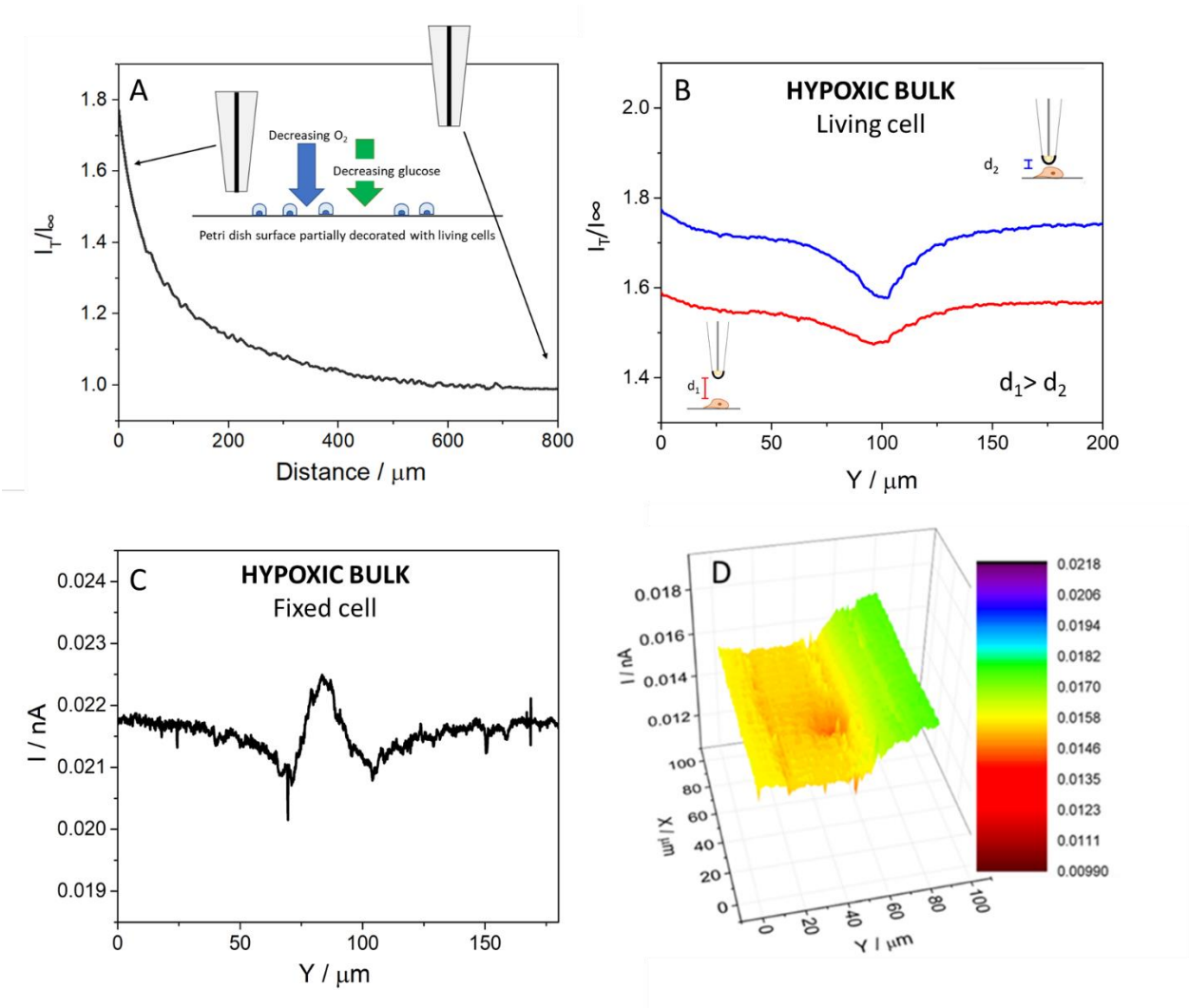


**Fig. 5.** a) SECM approach curve towards the bare surface of the Petri dish containing MDA-MB-468 cells, recorded with the PPyr-GOx-PBT-modified Pt ME in normoxic DMEM culture medium containing 5.5 mM glucose. b) Horizontal SECM line scans over a MDA-MB-468 cell at two different working distances ($d_1$ = 18 µm and $d_2$ = 16 µm from the Petri dish bottom) under hypoxic conditions. c) Horizontal SECM line scan over a fixed MDA-MB-468 cell under hypoxic conditions ($d$ = 20 µm from the Petri dish bottom). d) SECM image (x,y-plane) in constant height of the single cell. $E_T$ = +0.75 V vs. Ag quasi-RE. CE = Pt wire.

Thereafter, the micro-biosensor was positioned with working distances $d_1$ = 18 µm and $d_2$ = 16 µm above the bottom of the Petri dish and scanned in constant height over a single adhered MDA-MB-468 cell to detect the cellular consumption of glucose (**Fig. 5b**). Over the cell, the recorded current decreases due to the consumption of glucose by tumor cell metabolic activity that decreases the glucose concentration locally in the surroundings of the cell. Notably, when the working distance is reduced, the micro-biosensor response improves: the oxidation current over the bare

Petri dish surface increase due to limited oxygen availability while, at the same time, the spatial resolution of the cell glucose consumption profile increases. The latter is shown by the more pronounced decrease of current over the cell for $d_2$ compared to $d_1$. As well known, SECM measurements carried out in constant height mode over cells are subject to their topographical contribution affecting the real working distance. This constitutes a relevant component of current variations during the scans. When scanning over a cell the probe-to-substrate distance decreases due to the 3D shape of the cell, an increase of current should be detected, in case the glucose concentration would be indifferent, when scanning over the cell due to its topographical contribution (see discussion *vide supra*). However, a clear drop in the recorded signal is seen when the micro-biosensor is laterally moved at constant height above the adhered cell, which is clearly caused by cellular glucose consumption and not by topographical contribution. The topographical contribution to the SECM line scans was verified by performing a line scan over a fixed cell, thus a cell without metabolic activity. As it can be seen in **Fig. 5c**, the current remained nearly constant. Just above the center of the living cell, where the working distance was the smallest, a minor increase of the sensor response due to the decreased working distance and reduced oxygen concentration can be noted, in agreement with the observation described *vide supra*. Based on this result, it can be concluded that the topographic contribution compared to the signal changes caused by local variations in glucose concentrations is minor (**Scheme S9**). The stability of the micro-biosensor was then demonstrated performing an SECM image (*x*,*y*-plane) in constant height of the single cell (**Fig. 5d**).

## 3. Conclusions

To conclude, we have prepared in a one-step process an enzymatic glucose micro-biosensor that enabled the detection of glucose as one important metabolic tumor marker in the oxygen-depleted environment. This was tested for MDA-MB-468 cancer cells from breast metastatic adenocarcinoma. The micro-biosensor was electrochemically fabricated under optimized conditions via the electro-polymerization of pyrrole. During the anodic process, the formation of positively charged polymer entities resulted in the electrostatic entrapment of glucose oxidase and of iron redox species, such as ferricyanide. The results of electrochemical characterizations of the prepared micro-biosensor under hypoxic and normoxic conditions suggests a mixed detection

mechanism, which is based on the mediation of electrons between glucose oxidase and the electrode via the ferrocyanide/ferricyanide redox couple and by the presence of a Prussian Blue type material electrocatalyzing the conversion of hydrogen peroxide. A Prussian Blue type material is only indirectly seen in the measurements, for instance by specific catalytic electrode reactions, because cyclic voltammograms, recorded with the functionalized electrode, do not clearly demonstrate redox peaks that are typical for Prussian blue and its derivatives. The presence of ferrocyanide/ferricyanide can be also suggested. With the as-prepared glucose micro-biosensor linear calibration lines in the range of 1 mM to 7 mM of glucose were created, giving under hypoxic conditions a LOD below 1 mM and sensitivities 3.4 and 2.3 times higher compared to identically prepared micro-biosensors without the Prussian Blue type material and compared to the micro-biosensor performance under normoxic conditions, respectively. SECM measurements of glucose in the microenvironment of individual cells demonstrated the potential of the present glucose microsensor to study the spatial metabolic features of tumors in the frequent hypoxic environments in the tumor masses. Our measurements document the activity of the glycolytic metabolism of cancer cells under hypoxic conditions. The application as SECM probe enabled glucose measurements with high spatial resolution in order to image the profile of the cellular glycolytic activity of single cancer cells. The correlation between hypoxic conditions and the glycolytic metabolism of cancer cells may also be a decisive marker in tumor prognosis in which the increased invasiveness and enhanced drug resistance are often correlated to hypoxia in cancer.

## Acknowledgements

This work was supported by Fondazione AIRC per la Ricerca sul Cancro (MFAG Id. 19044) and Ministero della Salute GR-2018-12367747. We thank Sara Stagni for helping in preliminary results.

## References

[1] M.G.V. Heiden, L.C. Cantley, C.B. Thompson, Understanding the warburg effect: The metabolic requirements of cell proliferation, Science (80-. ). 324 (2009) 1029–1033. https://doi.org/10.1126/science.1160809.

[2] M. V. Liberti, J.W. Locasale, The Warburg Effect: How Does it Benefit Cancer Cells?, Trends Biochem. Sci. 41 (2016) 211–218. https://doi.org/10.1016/j.tibs.2015.12.001.

[3] G.H. Heppner, B.E. Miller, Tumor heterogeneity: biological implications and therapeutic

consequences, Cancer Metastasis Rev. 2 (1983) 5–23. https://doi.org/10.1007/BF00046903.

[4] H. Axelson, E. Fredlund, M. Ovenberger, G. Landberg, S. Påhlman, Hypoxia-induced dedifferentiation of tumor cells - A mechanism behind heterogeneity and aggressiveness of solid tumors, Semin. Cell Dev. Biol. 16 (2005) 554–563. https://doi.org/10.1016/j.semcdb.2005.03.007.

[5] M. Robertson-Tessi, R.J. Gillies, R.A. Gatenby, A.R.A. Anderson, Impact of metabolic heterogeneity on tumor growth, invasion, and treatment outcomes, Cancer Res. 75 (2015) 1567–1579. https://doi.org/10.1158/0008-5472.CAN-14-1428.

[6] K.L. Eales, K.E.R. Hollinshead, D.A. Tennant, Hypoxia and metabolic adaptation of cancer cells, Oncogenesis. 5 (2016) e190–e190. https://doi.org/10.1038/oncsis.2015.50.

[7] J.G. Rajendran, D.A. Mankoff, F. O'Sullivan, L.M. Peterson, D.L. Schwartz, E.U. Conrad, A.M. Spence, M. Muzi, D.G. Farwell, K.A. Krohn, Hypoxia and Glucose Metabolism in Malignant Tumors: Evaluation by [ 18F]Fluoromisonidazole and [18F]]Fluorodeoxyglucose Positron Emission Tomography Imaging, Clin. Cancer Res. 10 (2004) 2245–2252. https://doi.org/10.1158/1078-0432.CCR-0688-3.

[8] T.G. Lohith, T. Kudo, Y. Demura, Y. Umeda, Y. Kiyono, Y. Fujibayashi, H. Okazawa, Pathophysiologic correlation between 62Cu-ATSM and 18F-FDG in lung cancer, J. Nucl. Med. 50 (2009) 1948–1953. https://doi.org/10.2967/jnumed.109.069021.

[9] G.L. Semenza, Hypoxia-inducible factors in physiology and medicine, Cell. 148 (2012) 399–408. https://doi.org/10.1016/j.cell.2012.01.021.

[10] D.A. Chan, A.J. Giaccia, Hypoxia, gene expression, and metastasis, Cancer Metastasis Rev. 26 (2007) 333–339. https://doi.org/10.1007/s10555-007-9063-1.

[11] M. Höckel, P. Vaupel, Tumor hypoxia: Definitions and current clinical, biologic, and molecular aspects, J. Natl. Cancer Inst. 93 (2001) 266–276. https://doi.org/10.1093/jnci/93.4.266.

[12] L. Li, D.R. Walt, Dual-Analyte Fiber-Optic Sensor for the Simultaneous and Continuous Measurement of Glucose and Oxygen, Anal. Chem. 67 (1995) 3746–3752. https://doi.org/10.1021/ac00116a021.

[13] A. Pasic, H. Koehler, I. Klimant, L. Schaupp, Miniaturized fiber-optic hybrid sensor for continuous glucose monitoring in subcutaneous tissue, Sensors Actuators, B Chem. 122 (2007) 60–68. https://doi.org/10.1016/j.snb.2006.05.010.

[14] O.S. Wolfbeis, I. Oehme, N. Papkovskaya, I. Klimant, Sol-gel based glucose biosensors employing optical oxygen transducers, and a method for compensating for variable oxygen background, Biosens. Bioelectron. 15 (2000) 69–76. https://doi.org/10.1016/S0956-5663(99)00073-1.

[15] J. Wang, Sol-gel materials for electrochemical biosensors, Anal. Chim. Acta. 399 (1999) 21–27. https://doi.org/10.1016/S0003-2670(99)00572-3.

[16] E.W. Nery, M. Kundys, P.S. Jeleń, M. Jönsson-Niedziólka, Electrochemical glucose sensing: Is there still room for improvement?, Anal. Chem. 88 (2016) 11271–11282. https://doi.org/10.1021/acs.analchem.6b03151.

[17] A. Soldà, G. Valenti, M. Marcaccio, M. Giorgio, P.G. Pelicci, F. Paolucci, S. Rapino, Glucose and Lactate Miniaturized Biosensors for SECM-Based High-Spatial Resolution Analysis: A Comparative Study, ACS Sensors. 2 (2017) 1310–1318. https://doi.org/10.1021/acssensors.7b00324.

[18] D.W. Kimmel, G. Leblanc, M.E. Meschievitz, D.E. Cliffel, Electrochemical sensors and biosensors, Anal. Chem. 84 (2012) 685–707. https://doi.org/10.1021/ac202878q.

[19] A. Kausaite-Minkstimiene, V. Mazeiko, A. Ramanaviciene, Y. Oztekin, A. OsmanSolak, A. Ramanavicius, Evaluation of Some Redox Mediators in the Design of Reagentless Amperometric Glucose Biosensor, Electroanalysis. 26 (2014) 1528–1535. https://doi.org/10.1002/elan.201400023.

[20] H.J. Hecht, H.M. Kalisz, J. Hendle, R.D. Schmid, D. Schomburg, Crystal structure of glucose oxidase from Aspergillus niger refined at 2.3 Å reslution, J. Mol. Biol. 229 (1993) 153–172. https://doi.org/10.1006/jmbi.1993.1015.

[21] P. Janda, J. Weber, Quinone-mediated glucose oxidase electrode with the enzyme immobilized in polypyrrole, J. Electroanal. Chem. 300 (1991) 119–127. https://doi.org/10.1016/0022-0728(91)85388-6.

[22] D.V. Estrada-Osorio, R.A. Escalona-Villalpando, A. Gutiérrez, L.G. Arriaga, J. Ledesma-García, Poly-L-lysine-modified with ferrocene to obtain a redox polymer for mediated glucose biosensor application, Bioelectrochemistry. 146 (2022) 108147. https://doi.org/10.1016/j.bioelechem.2022.108147.

[23] S.F. Hou, K.S. Yang, H.Q. Fang, H.Y. Chen, Amperometric glucose enzyme electrode by immobilizing glucose oxidase in multilayers on self-assembled monolayers surface, Talanta. 47 (1998) 561–567. https://doi.org/10.1016/S0039-9140(98)00081-2.

[24] P. Wang, S. Amarasinghe, J. Leddy, M. Arnold, J.S. Dordick, Enzymatically prepared poly(hydroquinone) as a mediator for amperometric glucose sensors, Polymer (Guildf). 39 (1998) 123–127. https://doi.org/10.1016/S0032-3861(97)00228-0.

[25] M. Şenel, Construction of reagentless glucose biosensor based on ferrocene conjugated polypyrrole, Synth. Met. 161 (2011) 1861–1868. https://doi.org/10.1016/j.synthmet.2011.06.025.

[26] K. Itaya, I. Uchida, S. Toshima, Catalysis of the Reduction of Molecular Oxygen at Mixed Valence Complex Modified Electrodes of Prussian Blue Analogs, Nippon Kagaku Kaishi. 1984 (1984) 1849–1853. https://doi.org/10.1246/nikkashi.1984.1849.

[27] J. Estelrich, M.A. Busquets, Prussian Blue: A Nanozyme with Versatile Catalytic Properties, Int. J. Mol. Sci. 22 (2021) 5993. https://doi.org/10.3390/ijms22115993.

[28] R. Garjonyte, A. Malinauskas, Operational stability of amperometric hydrogen peroxide sensors, based on ferrous and copper hexacyanoferrates, Sensors Actuators B Chem. 56 (1999) 93–97. https://doi.org/10.1016/S0925-4005(99)00161-6.

[29] L. Zhu, J. Zhai, Y. Guo, C. Tian, R. Yang, Amperometric Glucose Biosensors Based on Integration of Glucose Oxidase onto Prussian Blue/Carbon Nanotubes Nanocomposite Electrodes, Electroanalysis. 18 (2006) 1842–1846. https://doi.org/10.1002/elan.200603594.

[30] G. Fu, X. Yue, Z. Dai, Glucose biosensor based on covalent immobilization of enzyme in sol–gel composite film combined with Prussian blue/carbon nanotubes hybrid, Biosens. Bioelectron. 26 (2011) 3973–3976. https://doi.org/10.1016/j.bios.2011.03.007.

[31] S. Yang, Y. Lu, P. Atanossov, E. Wilkins, X. Long, Microfabricated glucose biosensor with glucose oxidase entrapped in sol- gel matrix, Talanta. 47 (1998) 735–743. https://doi.org/10.1016/S0039-9140(98)00119-2.

[32] B.A. Gregg, A. Heller, Cross-Linked Redox Gels Containing Glucose Oxidase for Amperometric Biosensor Applications, Anal. Chem. 62 (1990) 258–263. https://doi.org/10.1021/ac00202a007.

[33] P.-C. Nien, T.-S. Tung, K.-C. Ho, Amperometric Glucose Biosensor Based on Entrapment of Glucose Oxidase in a Poly(3,4-ethylenedioxythiophene) Film, Electroanalysis. 18 (2006) 1408–1415. https://doi.org/10.1002/elan.200603552.

[34] G. Fortier, E. Brassard, D. Bélanger, Optimization of a polypyrrole glucose oxidase biosensor, Biosens. Bioelectron. 5 (1990) 473–490. https://doi.org/10.1016/0956-5663(90)80036-D.

[35] D. Bélanger, J. Nadreau, G. Fortier, Electrochemistry of the polypyrrole glucose oxidase electrode, J. Electroanal. Chem. 274 (1989) 143–155. https://doi.org/10.1016/0022-0728(89)87036-6.

[36] A.I. Rekertaitė, A. Valiūnienė, P. Virbickas, A. Ramanavicius, Physicochemical Characteristics of Polypyrrole/(Glucose oxidase)/(Prussian Blue)-based Biosensor Modified with Ni- and Co-Hexacyanoferrates, Electroanalysis. 31 (2019) 50–57. https://doi.org/10.1002/elan.201800526.

[37] A. Valiūnienė, J. Petronienė, M. Dulkys, A. Ramanavičius, Investigation of Active and Inactivated Yeast Cells by Scanning Electrochemical Impedance Microscopy, Electroanalysis. 32 (2020) 367–374. https://doi.org/10.1002/elan.201900414.

[38] P.N. Bartlett, R.G. Whitaker, Electrochemical immobilisation of enzymes, J. Electroanal. Chem. Interfacial Electrochem. 224 (1987) 37–48. https://doi.org/10.1016/0022-0728(87)85082-9.

[39] T.-E. Lin, S. Rapino, H.H. Girault, A. Lesch, Electrochemical imaging of cells and tissues, Chem. Sci. 9 (2018) 4546–4554. https://doi.org/10.1039/C8SC01035H.

[40] P. Sun, F.O. Laforge, M. V. Mirkin, Scanning electrochemical microscopy in the 21st century, Phys. Chem. Chem. Phys. 9 (2007) 802–823. https://doi.org/10.1039/b612259k.

[41] M. Malferrari, M. Becconi, S. Rapino, Electrochemical monitoring of reactive oxygen/nitrogen species and redox balance in living cells, Anal. Bioanal. Chem. 411 (2019) 4365–4374. https://doi.org/10.1007/s00216-019-01734-0.

[42] G. Wittstock, M. Burchardt, S.E. Pust, Y. Shen, C. Zhao, Scanning electrochemical microscopy for direct imaging of reaction rates, Angew. Chemie - Int. Ed. 46 (2007) 1584–1617. https://doi.org/10.1002/anie.200602750.

[43] I. Abdel Aziz, M. Malferrari, F. Roggiani, G. Tullii, S. Rapino, M.R. Antognazza, Light-Triggered Electron Transfer between a Conjugated Polymer and Cytochrome C for Optical Modulation of Redox Signaling, IScience. 23 (2020) 101091. https://doi.org/10.1016/j.isci.2020.101091.

[44] S. Rapino, G. Valenti, R. Marcu, M. Giorgio, M. Marcaccio, F. Paolucci, Microdrawing and highlighting a reactive surface, J. Mater. Chem. 20 (2010) 7272–7275. https://doi.org/10.1039/c0jm00818d.

[45] L. Bartolini, M. Malferrari, F. Lugli, F. Zerbetto, F. Paolucci, P.G. Pelicci, C. Albonetti, S. Rapino, Interaction of Single Cells with 2D Organic Monolayers: A Scanning Electrochemical Microscopy Study, ChemElectroChem. 5 (2018) 2975–2981. https://doi.org/10.1002/celc.201800731.

[46] M. Malferrari, A. Ghelli, F. Roggiani, G. Valenti, F. Paolucci, M. Rugolo, S. Rapino, Reactive Oxygen Species Produced by Mutated Mitochondrial Respiratory Chains of Entire Cells Monitored Using Modified Microelectrodes, ChemElectroChem. 6 (2019) 627–633. https://doi.org/10.1002/celc.201801424.

[47] R. Borghese, M. Malferrari, M. Brucale, L. Ortolani, M. Franchini, S. Rapino, F. Borsetti, D. Zannoni, Structural and electrochemical characterization of lawsone-dependent production of tellurium-metal nanoprecipitates by photosynthetic cells of Rhodobacter capsulatus, Bioelectrochemistry. 133 (2020) 107456. https://doi.org/10.1016/j.bioelechem.2020.107456.

[48] S. Rapino, R. Marcu, A. Bigi, A. Soldà, M. Marcaccio, F. Paolucci, P.G. Pelicci, M. Giorgio, Scanning electro-chemical microscopy reveals cancer cell redox state, Electrochim. Acta. 179 (2015) 65–73. https://doi.org/10.1016/j.electacta.2015.04.053.

[49] J. Petroniene, I. Morkvenaite- Vilkonciene, R. Miksiunas, D. Bironaite, A. Ramanaviciene, L. Mikoliunaite, A. Kisieliute, K. Rucinskas, V. Janusauskas, I. Plikusiene, S. Labeit, A. Ramanavicius, Evaluation of Redox Activity of Human Myocardium- derived Mesenchymal Stem Cells by Scanning Electrochemical Microscopy, Electroanalysis. 32 (2020) 1337–1345. https://doi.org/10.1002/elan.201900723.

[50] G.G. Wallace, P.R. Teasdale, G.M. Spinks, L.A.P. Kane-Maguire, Conductive Electroactive Polymers, CRC Press, 2008. https://doi.org/10.1201/9781420067156.

[51] N.F. Almeida, E.J. Beckman, M.M. Ataai, Immobilization of glucose oxidase in thin polypyrrole films: Influence of polymerization conditions and film thickness on the activity and stability of the immobilized enzyme, Biotechnol. Bioeng. 42 (1993) 1037–1045. https://doi.org/10.1002/bit.260420904.

[52] M.-H. Xue, Q. Xu, M. Zhou, J.-J. Zhu, In situ immobilization of glucose oxidase in chitosan–gold nanoparticle hybrid film on Prussian Blue modified electrode for high-sensitivity glucose detection, Electrochem. Commun. 8 (2006) 1468–1474. https://doi.org/10.1016/j.elecom.2006.07.019.

[53] R. Yang, Z. Qian, J. Deng, Electrochemical Deposition of Prussian Blue from a Single Ferricyanide Solution, J. Electrochem. Soc. 145 (1998) 2231–2236. https://doi.org/10.1149/1.1838625.

[54] D. Zhang, K. Wang, D.C. Sun, X.H. Xia, H.-Y. Chen, Ultrathin Layers of Densely Packed Prussian Blue Nanoclusters Prepared from a Ferricyanide Solution, Chem. Mater. 15 (2003) 4163–4165. https://doi.org/10.1021/cm034594r.

[55] Y. Fu, C. Chen, Q. Xie, X. Xu, C. Zou, Q. Zhou, L. Tan, H. Tang, Y. Zhang, S. Yao, Immobilization of Enzymes through One-Pot Chemical Preoxidation and Electropolymerization of Dithiols in Enzyme-Containing Aqueous Suspensions To Develop Biosensors with Improved Performance, Anal. Chem. 80 (2008) 5829–5838. https://doi.org/10.1021/ac800178p.

[56] A. Abbaspour, M.A. Kamyabi, Electrochemical formation of Prussian blue films with a single ferricyanide solution on gold electrode, J. Electroanal. Chem. 584 (2005) 117–123. https://doi.org/10.1016/j.jelechem.2005.07.008.

[57] R. Venugopal, B.A. Saviue, The effect of oxygen upon the kinetics of glucose oxidase inactivation, Can. J. Chem. Eng. 71 (1993) 917–924. https://doi.org/10.1002/cjce.5450710613.

[58] Z. Tang, R.F. Louie, J.H. Lee, D.M. Lee, E.E. Miller, G.J. Kost, Oxygen effects on glucose meter measurements with glucose dehydrogenase- and oxidase-based test strips for point-of-care testing, Crit. Care Med. 29 (2001) 1062–1070. https://doi.org/10.1097/00003246-200105000-00038.